



Article

Characterization of Lignocellulose Nanofibril from Desilicated Rice Hull with Carboxymethylation Pretreatment

Audrey Zahra ¹, Seo-Kyoung Lim ² and Soo-Jeong Shin ^{1,2,*}

¹ Department of Forest Product, Chungbuk National University Graduate School, Cheongju 28644, Chungbuk, Republic of Korea; audreyzahra@chungbuk.ac.kr

² Nature Costech Inc., Cheongju 28578, Chungbuk, Republic of Korea; lsk.nacostech@gmail.com

* Correspondence: soojshin@chungbuk.ac.kr

Abstract: Rice hulls have a high-value potential, and the lignocellulose components are underutilized compared to other biomass resources. Pretreatments such as carboxymethylation of the degree of substitutions (DS) are used to prepare lignocellulose nanofibril (LCNF) from desilicated rice hull (DSRH). High-pressure homogenization (HPH) and grinding are used to process nano fibrillation. The composition of LCNF DS of desilicated rice hull was identified using ¹H NMR for polysaccharide composition and DS determination, acetone and hot water extraction to evaluate extractives, and Klason lignin for lignin content. LCNF was prepared using various DS from 0.2 until DS 0.4. The results showed that LCNF DS has a more than −30 mV zeta potential, suitable for stable nanoemulsion formulations. The particle size of LCNF DS decreases with an increasing carboxyl content in the hydrogel and an increasing number of passes through grinding and high-pressure homogenization, of which LCNF DS 0.4 had the smallest width and length. Mechanical processes further reduced the size.

Keywords: rice hull; carboxymethylation; lignin; lignocellulose nanofibril; hydrogel



Citation: Zahra, A.; Lim, S.-K.; Shin, S.-J. Characterization of Lignocellulose Nanofibril from Desilicated Rice Hull with Carboxymethylation Pretreatment. *Polysaccharides* **2024**, *5*, 16–27. <https://doi.org/10.3390/polysaccharides5010002>

Academic Editors: Valentina Siracusa, Nadia Lotti, Michelina Soccio and Alexey L. Iordanskii

Received: 12 December 2023

Revised: 12 January 2024

Accepted: 17 January 2024

Published: 22 January 2024



Copyright: © 2024 by the authors. Licensee MDPI, Basel, Switzerland. This article is an open access article distributed under the terms and conditions of the Creative Commons Attribution (CC BY) license (<https://creativecommons.org/licenses/by/4.0/>).

1. Introduction

Biomass refers to all organisms, living or dead, including plants, algae, and animals. Among these, plants are the primary source of biomass [1]. Plant biomass comprises several crucial elements, such as cellulose, hemicelluloses, and lignin, as well as trace amounts of inorganic or extractive materials [2]. Photosynthesis is the primary source of glucose, which is the principal component of plant biomass [1,2]. Glucose is vital for the survival and growth of plants and serves as a crucial energy source for living organisms that rely on plants for sustenance [2].

Lignocellulose is a complex and highly abundant organic compound that is present in various types of biomass, such as trees, grasses, and agricultural residues [3]. It is a vital component of plant cell walls, providing structural support and protection against mechanical stresses and pathogens. Lignocellulose is composed of three primary polymers, namely cellulose, hemicellulose, and lignin [4]. Lignocellulose is a valuable and renewable resource that can be converted into a wide range of biofuels, chemicals, and materials. It can be sourced from different types of biomass, including wood, agricultural residues, and energy crops [5,6]. Cellulose, the most abundant natural organic material, is formed by glucose through a β -1,4-linkage to the homopolymer [1]. It exhibits both crystalline and paracrystalline regions, with the crystalline region displaying higher resistance to chemical or biological attacks than the paracrystalline region. Cellulose bundles are organized from elementary fibrils to microfibrils and macrofibrils as integral components of the cell wall [2]. Hemicelluloses, categorized into glucomannan and xylan, play crucial roles. Glucomannan is the predominant hemicellulose in softwood, with a galactose/glucose/mannose ratio of 1:1:3 (galactoglucomannan) or 0.1:1:4 (glucomannan). Glucuronoxylan, the primary

hemicellulose in hardwood, annual plants, or perennial plants, contains glucuronic acid as a side chain [2,5]. Lignin, present in softwood as coniferyl alcohol monomers and in hardwood as a combination of coniferyl alcohol and sinapyl alcohol repeating units, serves a vital role in biomass by providing structural building blocks and protecting against external factors. In annual or perennial plants, p-hydroxy coumaryl alcohol plays a significant role in lignin, contributing to its overall function in the plant's structure and resilience [3–6].

Rice hull is a good biomass resource with similar cellulose, hemicelluloses, and lignin content to softwood, hardwood, or grasses. Rice hull is a protective outer layer of rice grains which is separated from rice by mechanical action as generated as residual biomass in the rice polishing process [7,8]. However, they are an excellent source of biomass for bioenergy and bioproducts, which could help reduce the environmental impact of rice production and provide a sustainable alternative to traditional fossil fuels [9]. Researchers have been exploring different ways to convert rice hulls into valuable products in recent years, such as biofuels, activated carbon, and nanocellulose [8,9]. By utilizing rice hulls as a renewable and sustainable resource, we could make significant strides towards achieving a greener and more sustainable future.

For cellulose nanofibril (CNF) production, lignocellulosic biomass needed delignification by pulping or bleaching. Significant amounts of hemicelluloses and lignin from raw materials such as wood are removed as soluble products during the process of making cellulose through pulping and bleaching [10]. Pulping reactions are those from the hydrolysis of the lignin polymer structure to monomeric degradation assisted by acid or base [10,11]. Bleaching of lignin causes the degradation of lignin to fragments by oxidation of lignin. Chlorine dioxide, oxygen, and hydrogen peroxide are typical bleaching chemicals. The most expensive part of this chemical pulping process is the combined heat and power (electric) system in the recovery boiler which acts as a hindrance in producing cellulose from non-normal biomass [11]. Therefore, chemical pretreatment is a viable method for achieving nano fibrillation in cellulosic materials, as it reduces the energy required for the process. Carboxymethylation and TEMPO-oxidation are the most commonly used chemical pretreatment methods [12,13]. After pretreatment, cellulose material was nanofibrillated by the mechanical process using a grinding by supermass-collider or high-pressure homogenization processes [14,15]. The quality of produced cellulose nanofiber could be controlled by particle size analysis, measuring the water retention value by centrifuge, and measuring rheological properties by rheometer [16–18]. Employing these techniques can effectively produce high-quality nanofibrils [18].

Cellulose nanofibrils are tiny fibrils with strong hydrophilic properties, making mixing them with hydrophobic materials challenging [19]. Recent research has shown that incorporating lignin, an intricate organic polymer found in plant cell walls, into nanofibrils can improve their blending capabilities with less hydrophilic materials. This is because lignin-containing nanofibers have lower hydrophilicity than pure cellulose, which is capable of producing biodegradable composite materials, which have promising applications for the replacement of petroleum-derived materials [19,20]. Scientific inquiry has demonstrated that lignin-containing nanofibers have the potential to be an excellent substitute for blending with less hydrophilic materials. Therefore, the incorporation of LCNF into the nanocomposite matrix is a superior strategy for fabricating various biodegradable materials such as nanocellulose-reinforced films, barrier materials, and hydrophobic composites. This discovery is particularly significant because it broadens the range of applications for cellulose nanofibril composites, especially in situations where hydrophobic materials are required [20].

Over the years, extensive research has been conducted on bleached cellulose nanofibrils (BCNF). Recently, researchers have paid attention to lignin-containing cellulose nanofibrils (LCNF) and their immense potential applications [21]. These nanofibrils are unique and have been integrated into various products as fillers and reinforcing agents in different matrices. LCNF have also shown significant improvements in strength and stiffness when used as additives in papermaking processes [22]. When utilizing lignin-containing

cellulose as the primary raw material for breaking down to lignocellulosic nanoscale fiber, there are two significant advantages [20]. First, due to the no delignification step, there is less environmental harm from chlorinated lignin, which is produced during the oxidative lignin removal process. Second, lignin contains some functional groups which contribute to the lignin some degree of hydrophobicity. These provide residual lignin in cellulose with adequate reactivity to modify the hydrophilicity and polarity of LCNF suspensions [19–21,23]. This, in turn, facilitates the dispersion and storage of LCNFs. The development of neat and composite LCNF films has opened new avenues for their use in packaging and other applications. Their potential applications also include barrier films, emulsions, and nanocomposites, as presented in a list of applications [23]. With the increasing interest in sustainable and eco-friendly materials, LCNF could play a significant role in meeting the demand for such materials due to their renewability, biodegradability, and cost-effectiveness.

This study provides a comprehensive overview of the research on LCNF obtained from desilicated rice hulls. It focuses on how the lignin component of LCNF affects its processing and characteristics. Additionally, the research investigates the impact of carboxymethylation pretreatment on lignin, chemical composition, calculated degree of substitution, and zeta potential in desilicated rice hulls. It also determines the particle size of LCNF after undergoing nano fibrillation through supermass-colloider milling and high-pressure homogenization (HPH). Accurately characterizing the properties of LCNF is critical in determining its potential in desilicated rice hulls.

2. Materials and Methods

2.1. Materials

This research study utilized a rice hull that underwent an alkaline extraction as a desilication process, which was previously explained in detail in a separate paper referenced [24]. The desilicated rice hull (DSRH) was implemented as a main component in the research. Chemicals for prepared lignocellulose nanofibril (LCNF) pretreatment were ethanol 94.5% ($\text{CH}_3\text{CH}_2\text{OH}$) from Samchun Pure Chemical Co., Ltd., Pyeongtaek, Republic of Korea; sodium hydroxide 98.0% (NaOH) from OCI Company Ltd., Seoul, Republic of Korea; and monochloroacetic acid 99.8% (MCA) from Denak Co., Ltd., Chiyoda, Japan. Chemical compositions were acetone 100% ($(\text{CH}_3)_2\text{CO}$) from Burdick & Jackson by SK Chemicals, Seongnam, Republic of Korea; sulfuric acid 95.0% (H_2SO_4) from Samchun Pure Chemical Co., Ltd., Pyeongtaek, Republic of Korea; deuterium oxide 99.9% (D_2O) from Sigma-Aldrich, Inc., St. Louis, MO, USA.

2.2. Preparation of LCNF Rice Hull in Different Degree of Substitution (DS)

In order to prepare Lignocellulose nanofibrils (LCNF) from DSRH with varying degrees of substitution (DS). A homogeneous solution was first prepared by dissolving NaOH in 200 mL of ethanol. Then, 30 g of dried DSRH was added to the solution, and the mixture was incubated at 30 °C and 200 rpm for 2 h. After that, a mixture of 20 mL of ethanol and MCA was added to the mixture, which was then left in a shaking incubator at 250 rpm and 30 °C for an hour. The reaction was carried out in an oven at 80 °C for 2 h. Next, the desilicated rice hull was subjected to a carboxymethyl substitution reaction to achieve the target DS of 0.2, 0.3, and 0.4 using NaOH (g) 4.44, 6.67, 8.89, and MCA (g) 4.33, 6.50, 8.67. Once the reaction was completed, the mixture was repeatedly washed and filtered with distilled water until a neutral pH was reached. Finally, the cellulose fiber was dried in the oven overnight and ground until smooth.

2.3. Preparation of Hydrogel LCNF Rice Hull with Various DS

The dried DSRH, which was subjected to carboxymethyl pretreatment, was added to distilled water to make a 2% suspension. The suspension was mixed with a homogenizer (IKA T25 Digital Ultra Turrax, Wertheim am Main, Germany) at 6500 rpm for 10 min. Then, a gel of 2% concentration of each LCNF DS was used to form nanofibrils by

combining grinding (Supermasscolloider; MKZA10-15IV, Masuko Sangyo, Kawaguchi-city, Saitama-pref, Japan) with conditions where a disk (MKG-C120#, Masuko Sangyo, Japan) gap of 200–250 μm with 1000 ± 50 rpm of disk rotation speed and high-pressure homogenizer (Panda PLUS 2000, GEA, Parma, Italy) with maintaining a pressure of 600 bar. The machines shown in Table 1 were passed through the treatment conditions.

Table 1. Combination of the degree of substitution, grinding, and high-pressure homogenization.

Degree of Substitution (DS)	Grinding (Passes)	High-Pressure Homogenization (Passes)
0.2	3	3
	6	6
	9	9
0.3	3	3
	6	6
	9	9
0.4	3	3
	6	6
	9	9

2.4. Analysis of Chemical Composition

The content of acetone extraction was measured using the TAPPI 204 om-88 method, while that of hot water extraction was determined by TAPPI 207 om-93. The TAPPI 222 om-88 method was used to analyze the acid-insoluble lignin.

The LCNF DS was dried and weighed at 0.02 g. It was then mixed with 0.6 mL of 72% H_2SO_4 and incubated at 30 °C for an hour. Following this, 3 mL of D_2O was added, and the mixture was placed in an oven at 100 °C for an hour. After cooling and filtering, the extractives were inserted into the NMR tube and processed using Bruker Avance 400 MHz ^1H [25,26]. The carbohydrate composition data was calculated based on the average of two replicates for each sample.

2.5. Analysis of Degree of Substitution after Carboxymethylation Treatment

The analysis was conducted using a Bruker Avance ^1H NMR spectrometer (400 MHz), and the anomeric hydrogen peak and the carboxyl group peak on the spectrum were integrated using the Topspin program. The degree of substitution of desilicated rice hull pretreated with carboxymethylation was calculated by substituting the integrated value of DS partial position 2, 3, and 6 with α,β glucose anomeric peak area in chemical shift [27].

2.6. Zeta Potential

LCNF DS samples for zeta potential were prepared by diluting the sample with distilled water to a concentration of 0.02%. The samples were then subjected to zeta potential measurements at 25 °C using Zetasizer Nano ZS (Malvern, Worcestershire, UK). Zeta potential data for each sample were calculated based on the average of three replicate experiments.

2.7. Nanoparticles Analysis

LCNF DS samples for nanoparticle analysis were prepared by diluting CNF with distilled water to a concentration of 0.02%, followed by treatment with Zetasizer Nano ZS (Malvern, Worcestershire, UK) at 25 °C. Size distribution results were generated by averaging 10 consecutive measurements of 12 10s runs as specified in ISO22412,2008 [28]. The results of cumulative analysis (z-ave, PdI) and intensity-based PSD analysis.

3. Result and Discussion

3.1. Carbohydrate Compositional Analysis of Various LCNF DS Desilicated Rice Hulls

Table 2 provides information regarding the chemical composition of desilicated rice hulls after carboxymethylation pretreatment. It was observed that an increase in carboxyl concentration led to a decrease in yield and hot water extraction, while acetone extraction and lignin increased. Rice hulls or straws have high silicate content that makes it difficult to process LCNF rice hulls mechanically. To solve this issue, desilication by alkali treatment was carried out, according to a previously published study. The desilicated rice hull had 0.2% acetone extraction, 5.9% hot water extraction, 10.0% lignin, 29.4% cellulose, 9.4% xylan, and 2.2% of inorganics [24]. Meanwhile, rice hull composition that has not undergone silica removal contains 28.7–35.62% cellulose, 11.96–29.3% hemicellulose, 15.38–20% lignin, and 17–18.71% ash/silica [29]. Rice hull after alkaline hydrogen peroxide treatment from Banyumas (Indonesia) contains cellulose (35%), hemicellulose (25%), lignin (20%), and ash (17%) [30]. Raw rice hull from a paddy field located in Isla Mayor (Seville, Spain) has acetone extractives 4.3%, methanol extractives 1.9%, water-soluble material 4.5%, Klason lignin 20.0%, acid-soluble lignin 2.5%, hemicellulose 28.3%, cellulose 27.2%, proteins 0.7%, and ash 10.6% [31].

Table 2. Chemical composition of desilicated rice hull LCNF with various DS (%).

Sample	Yield	Extractives		Lignin	Polysaccharide
		Acetone	Hot Water		
DSRH DS 0.2	84.63	3.80	6.57	10.50	63.76
DSRH DS 0.3	81.49	4.36	5.67	11.23	60.23
DSRH DS 0.4	78.68	5.62	4.11	12.02	56.93

In Figure 1, a typical spectrum resulting from ^1H NMR analysis of carboxymethylated desilicated rice hull is presented. Monosaccharide composition was measured and calculated by ^1H -NMR spectroscopy in the anomeric hydrogen and the carboxymethyl proton peak area chemical shift regions of 4.5–5.5 ppm [26,27]. It can be observed that the sugar peaks are well separated, and the peaks for glucose and xylose are dominant. The anomeric protons were converted to data for the carbohydrate composition in carboxymethylated DSRH, and the results are listed in Table 3. It was revealed through detailed investigations using ^1H NMR spectroscopy that the order of reactivity degree of substitution was found to be O-2 > O-6 > O-3. The calculation of the degree of substitution in the samples is performed by integrating the carboxymethyl position in the chemical shift using formula (1), and the resulting data are presented in Table 4.

$$\text{DS} = \frac{A + B + C + D}{G\alpha + G\beta} \quad (1)$$

A, Peak of Carboxymethyl protons at the H-2 α Position;

B, Peak of Carboxymethyl protons at the H-2 β Position;

C, Peak of Carboxymethyl protons at the H-3 Position;

D, Peak of Carboxymethyl protons at the H-6 Position;

G α , Peak of Anomeric protons at the α -Glucose Position;

G β , Peak of Anomeric protons at the β -Glucose Position.

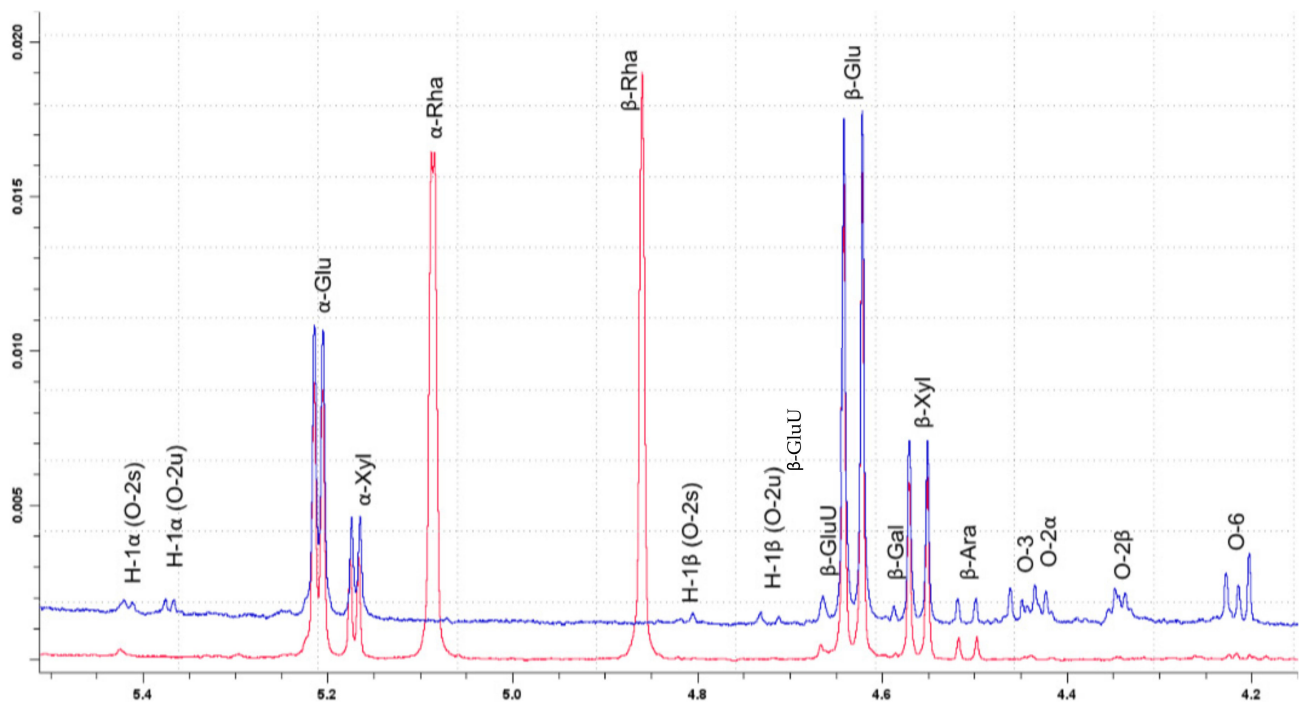


Figure 1. $^1\text{H-NMR}$ spectrum of monosaccharides from desilicated rice hull (red) and carboxymethylated desilicated rice hull (blue).

Table 3. Carbohydrate composition in desilicated rice hull LCNF DS samples (%).

Sample	Galactan	Glucuronic Acid	Arabinan	Cellulose	Xylan	Carboxymethyl
DSRH DS 0.2	3.76	1.35	1.39	72.82	17.65	2.79
DSRH DS 0.3	2.86	3.45	1.38	69.40	16.28	6.24
DSRH DS 0.4	1.65	6.34	1.20	66.83	15.56	8.14

Table 4. Degree of substitution of carboxymethylated desilicated rice hull by a $^1\text{H-NMR}$ method.

Target DS	Measured DS in DSRH
DS 0.2	0.17 ± 0.01
DS 0.3	0.27 ± 0.01
DS 0.4	0.38 ± 0.00

Based on the information in Table 3, the primary components of desilicated rice hull LCNF with different DS samples are cellulose and xylan. Interestingly, all monosaccharides decreased when the DS increased, except for glucuronic acid and galacturonic acid, which increased. Different pretreatments were applied to rice hull samples in a study conducted in Hebei province, China. The microwave-prepared sample had 93.70% solid recovery and contained 39.72% glucan, 17.61% xylan, 2.78% acetyl group, 15.80% ash, and 25.36% lignin. Meanwhile, the alkali-prepared sample had a 61.00% solid recovery rate and consisted of 49.45% glucan, 22.81% xylan, 2.85% ash, and 21.97% lignin. Lastly, the APCMP-prepared sample had 59.20% solid recovery and contained 49.77% glucan, 22.93% xylan, 2.75% ash, and 21.43% lignin [32].

3.2. Analysis of the Degree of Substitution of Carboxymethylated LCNF Desilicated Rice Hull

The effectiveness of the carboxymethylation pretreatment process is subject to the influence of both the reaction reagents and temperature [33]. Essentially, the hydroxyl group of cellulose is transformed into an anion with sodium hydroxide, and then chloroacetic acid reacts with the cellulose at that anion location. This results in the substitution of the hydroxyl group with a carboxymethyl group [34]. The quantity of carboxymethyl group present in cellulose after undergoing carboxymethylation pretreatment is a critical factor in determining the strength of the electrical repulsive force during the creation of nano cellulose. Therefore, it is vital to analyze the impact of pretreatment on the manufacturing process of nano cellulose, as explored in studies [33,35].

In this study, the LCNF was prepared according to the degree of carboxymethylation substitution required to confirm the nano fibrillation characteristics of DSRH, and carboxymethylated LCNF DSRH samples having a degree of substitution similar to the target degree of substitution were prepared. The anomeric hydrogen region of the NMR spectrum was used for quantitative analysis by integrating the peak area. Although the actual measured degree of substitution was lower than the target degree of substitution, it was confirmed through Table 4 that in all three cases, the degree of substitution was close to the target degree of substitution.

The degree of carboxymethylation pretreatment can be accurately assessed through the use of hydrogen nuclear magnetic resonance spectrum analysis, as shown in Figure 1 [27]. By examining the anomeric hydrogen peak of glucose, a sugar present in cellulose, and the hydrogen peak of the methyl group among the substituted carboxymethyl groups, the degree to which carboxymethyl groups replace hydrogen atoms in cellulose can be estimated with accuracy [8]. It is important to note that the positions in cellulose where carboxymethyl groups can substitute for hydrogen are limited to the 2nd, 3rd, and 6th carbon positions [27]. Furthermore, this method can also be used to determine the degree of methyl group substitution, allowing for a comprehensive analysis of the carboxymethylation process.

3.3. Zeta Potential of Various LCNF DS Desilicated Rice Hull

Zeta potential and surface charge density are essential factors that are closely related to the carboxyl group composition of each CNF [36]. Zeta potential is a measure of the electrostatic charge on the surface of a particle, while surface charge density is the total charge per unit area of the particle surface. These two factors play a crucial role in determining the dispersion stability of nanomaterials in their dispersion media [37]. In general, suspensions in water with zeta potential values that are the same as or greater than -30 mV are considered stable [38]. This is because high zeta potential values indicate a strong repulsive force between nanoparticles, which prevents them from aggregating and settling.

The zeta potential of desilicated rice hulls LCNF decreased as the DS increased from 0.2 (-36.2 mV) to DS 0.4 (-43.3 mV), as shown in Figure 2. This decrease in zeta potential is due to the increased carboxyl group composition. Similarly, carboxymethylated bleached rice hulls CNF exhibited the same decreasing trend as the DS increased from DS 0.2 (-49.1 mV) to DS 0.4 (-55.8 mV) [13]. However, the decrease in zeta potential is attributed to the varying compositions of these materials. Bleached rice hulls have no lignin and high cellulose purity, which means they lack the ability to attach with carboxyl groups. Additionally, they have more xylan content in the same sample weight, which affects the zeta potential and surface charge density. The difference in composition is the reason behind these variations. Bleached CNF from bleached kraft hardwood (HW) pulp received from Chungnam National University after TEMPO-oxidation had a -40 mV zeta potential [38].

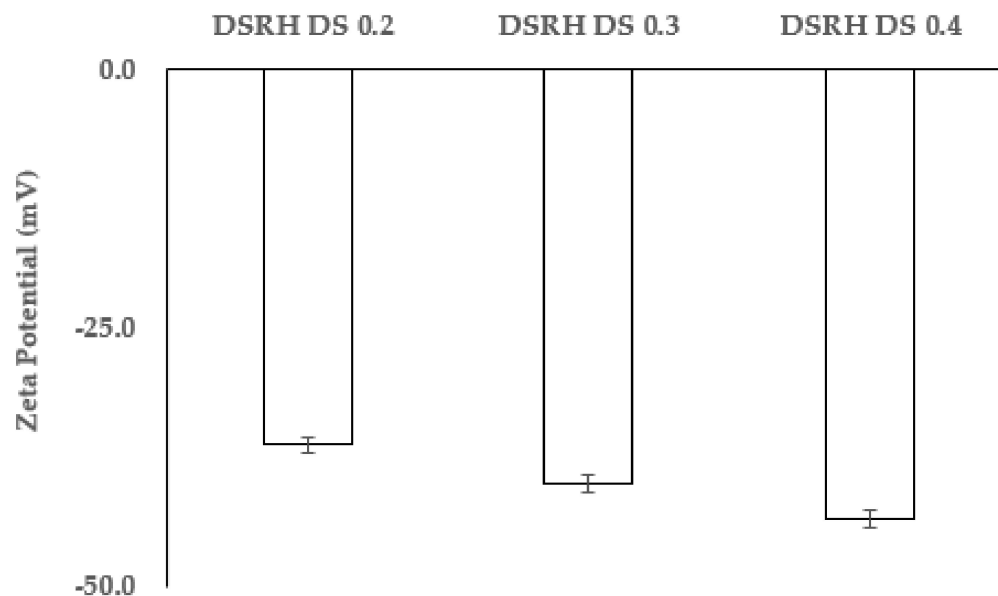


Figure 2. Zeta potential of different LCNF DS desilicated rice hull.

Understanding the relationship between zeta potential, surface charge density, and carboxyl group composition is crucial in developing stable nanomaterial dispersions. This knowledge can be used to optimize the properties of CNF for various applications, such as in the production of composites, coatings, and films.

3.4. Size of LCNF DS Desilicated Rice Hull

It is crucial to have a quick and easy method to measure the size of cellulose nanofibrils for quality control during the manufacturing process [39]. To characterize the cellulose nanofibrils, a nanoparticle size analyzer (dynamic laser scattering) was used, which revealed two distinct peak regions—one representing the width and the other representing the length of the nanofibrils [40]. Therefore, the dynamic laser scattering nanoparticle analysis is suggested as a quality control tool for estimating the length and width of cellulose nanofibers during fabrication [41].

The nanoparticle size analyzer used in the experiment uses the dynamic light scattering approach to determine particle size, as opposed to the laser diffraction method used in the colloidal particle size analyzer [40,42]. The laser diffraction method measures the particle size by analyzing the intensity of the light generated when a laser passes through a sample and the associated angle change [40,43].

The LCNF size was found to decrease with an increase in DS, grinding, and HPH, as shown in Table 5. The introduction of nanoparticle sorting by different treatments, such as DS, grinding, and HPH, made it possible to assess changes in the size of the hydrogel nanoparticles induced by the combination of those treatments, which is critical for quality control and regulatory compliance.

Cellulose nanofibers are rod or linear structures with varying widths and lengths. Typically, their width is several tens of nanometers, while their length spans from hundreds to thousands of nanometers [44]. These nanofibers possess a considerable aspect ratio and can be found in varying widths and lengths [45]. Their application in nanoparticle size analysis has proven helpful in numerous scenarios, as it can produce multiple particle size distributions instead of just one [46].

Table 5. The LCNF desilicated rice hull particle size in different DS, grinding, and HPH.

Sample	Grinding	HPH	Width (nm)	Length (nm)
DSRH DS 0.2	3	3	890.0 ± 39.5	1792.0 ± 28.2
		6	220.0 ± 16.1	692.9 ± 52.8
		9	56.3 ± 4.3	345.0 ± 47.2
	6	3	138.5 ± 31.1	622.6 ± 69.9
		6	92.1 ± 7.3	456.2 ± 5.9
		9	48.0 ± 8.0	164.3 ± 16.1
	9	3	99.3 ± 4.1	353.5 ± 41.2
		6	73.1 ± 4.3	287.9 ± 8.1
		9	56.7 ± 4.4	246.3 ± 14.9
DSRH DS 0.3	3	3	355.7 ± 32.4	1523.3 ± 69.0
		6	157.7 ± 23.9	663.1 ± 27.9
		9	144.1 ± 29.0	317.9 ± 8.8
	6	3	98.0 ± 18.6	592.4 ± 24.0
		6	73.0 ± 4.5	428.9 ± 22.9
		9	30.1 ± 10.3	151.0 ± 33.4
	9	3	92.6 ± 5.9	442.8 ± 29.9
		6	66.4 ± 4.8	344.4 ± 28.6
		9	53.7 ± 3.5	286.2 ± 8.5
DSRH DS 0.4	3	3	125.3 ± 2.6	524.0 ± 25.9
		6	48.7 ± 5.7	327.1 ± 11.4
		9	37.6 ± 4.3	156.3 ± 36.8
	6	3	111.3 ± 9.0	518.5 ± 49.8
		6	96.8 ± 15.2	393.4 ± 29.3
		9	40.9 ± 4.7	116.6 ± 26.0
	9	3	83.9 ± 3.5	408.0 ± 13.6
		6	34.2 ± 2.7	276.3 ± 3.3
		9	20.0 ± 1.2	115 ± 15.7

In the case of desilicated rice hull LCNF, those with a DS of 0.4 had smaller particles compared to those with a DS of 0.3 and 0.2. Similarly, grinding and high-pressure homogenization (HPH) at 9 had smaller particles than grinding and HPH at 3 and 6. The smallest particle was obtained from LCNF desilicated rice hull with a DS of 0.4, grinding of 9, and HPH of 9. This trend has also been observed with the carboxymethylation of bleached rice hull—an increased DS and grinding resulted in decreased size [14]. On the other hand, bagasse CNF from Australia, which was produced by ball milling, had a length of 2000 nm and a diameter of 50 nm [47]. TEMPO CNF from bleached kraft hardwood pulp had an original width of 3.5 ± 2.0 nm and length of 671.7 ± 961.2 nm, while homogeneous CNF had a width of 2.0 ± 0.6 nm and length of 639 ± 387.3 nm [38].

CNF from hardwood bleached kraft pulp provided by a company called M was produced through different combinations of grinder (G) and high-pressure homogenizer (H)—G2H4, G6H4, G8H4, and G8H10. These samples showed a similar trend in particle size distribution by nanoparticle analyzer (range size: 1.1–13.4 width and 36.7–266.7 length) and TEM (range size: 2.7–11.1 width and 99.1–669.1 length), with the smallest size obtained from G8H10 [40].

4. Conclusions

The substitution of the hydroxyl group to the carboxymethyl group in desilicated rice hull by pretreatment involved acetone and hot water extraction, lignin, glucuronic acid, galacturonic acid, galactan, arabinan, cellulose, and xylan. With increased carboxymethylation, the yield of the sample was decreased. LCNF can be used as nanofibril by carboxymethylation treatment with various DS, grinding, and HPH. The LCNF DSRH thus

produced had a width of 20–890 nm and a length of 115–1792 nm. Anionic addition increased with carboxymethylation pretreatment; it was found to affect increased cellulose, uronic acid, and arabinan but decreased galactan and xylan and also increased the negative charge of the zeta potential and decreased the size. The number of grinding and HPH operations also affects the particle size of the nanofibers. From the findings, DSRH, despite its high lignin content, can be transformed into LCNF. The optimization of LCNF properties can be achieved by regulating the degree of carboxymethylation pretreatment and the number of passes through milling and HPH. This approach eliminates the necessity of hazardous chemicals in the bleaching process. The ideal choice for LCNF is DS 0.4, as it exhibits the highest zeta potential and the smallest size, being as good as bleached CNF from hardwood.

Author Contributions: Investigation, A.Z. and S.-K.L.; validation, S.-K.L.; writing—original draft, A.Z. and S.-J.S.; writing—review and editing, S.-J.S. All authors have read and agreed to the published version of the manuscript.

Funding: This research received no external funding.

Institutional Review Board Statement: Not applicable.

Data Availability Statement: The data presented in this study are available in the article.

Conflicts of Interest: Author Seo-Kyoung Lim and Soo-Jeong Shin were employed by the company Nature Costech Inc. The remaining authors declare that the research was conducted in the absence of any commercial or financial relationships that could be construed as a potential conflict of interest.

References

1. Antar, M.; Lyu, D.; Nazari, M.; Shah, A.; Zhou, X.; Smith, D.L. Biomass for a sustainable bioeconomy: An overview of world biomass production and utilization. *Renew. Sustain. Energy Rev.* **2021**, *139*, 110691. [[CrossRef](#)]
2. Yang, C.; Lü, X. Composition of plant biomass and its impact on pretreatment. In *Advances in 2nd Generation of Bioethanol Production*; Woodhead Publishing: Cambridge, UK, 2021; pp. 71–85. [[CrossRef](#)]
3. Zhou, M.; Tian, X. Development of different pretreatments and related technologies for efficient biomass conversion of lignocellulose. *Int. J. Biol. Macromol.* **2022**, *202*, 256–268. [[CrossRef](#)] [[PubMed](#)]
4. Hemati, A.; Nazari, M.; Asgari Lajayer, B.; Smith, D.L.; Astatkie, T. Lignocellulosics in plant cell wall and their potential biological degradation. *Folia Microbiol.* **2022**, *67*, 671–681. [[CrossRef](#)] [[PubMed](#)]
5. Kumar, J.A.; Sathish, S.; Prabu, D.; Renita, A.A.; Saravanan, A.; Deivayanai, V.C.; Hosseini-Bandegharaei, A. Agricultural waste biomass for sustainable bioenergy production: Feedstock, characterization and pre-treatment methodologies. *Chemosphere* **2023**, *331*, 138680. [[CrossRef](#)] [[PubMed](#)]
6. Iglesias, M.C.; Gomez-Maldonado, D.; Via, B.K.; Jiang, Z.; Peresin, M.S. Pulping processes and their effects on cellulose fibers and nanofibrillated cellulose properties: A review. *For. Prod. J.* **2020**, *70*, 10–21. [[CrossRef](#)]
7. Papavasileiou, P.; Koutras, S.; Koutra, E.; Ali, S.S.; Kornaros, M. A novel rice hull-microalgal biorefinery for the production of natural phenolic compounds comprising of rice hull acid pretreatment and a two-stage *Botryococcus braunii* cultivation process. *Bioresour. Technol.* **2023**, *387*, 129621. [[CrossRef](#)] [[PubMed](#)]
8. Goodman, B.A. Utilization of waste straw and husks from rice production: A review. *J. Bioresour. Bioprod.* **2020**, *5*, 143–162. [[CrossRef](#)]
9. Singh, A.D.; Bakshi, P.; Kumar, P.; Kour, J.; Dhiman, S.; Ibrahim, M.; Bhardwaj, R. Effects of Agricultural Wastes on Environment and Its Control Measures. In *Agricultural and Kitchen Waste*; CRC Press: Boca Raton, FL, USA, 2022; pp. 219–239.
10. Balkissoon, S.; Andrew, J.; Sithole, B. Dissolving wood pulp production: A review. *Biomass Convers. Biorefin.* **2023**, *13*, 16607–16642. [[CrossRef](#)]
11. Damasceno, A.; Carneiro, L.; Andrade, N.; Vasconcelos, S.; Brito, R.; Brito, K. Simultaneous prediction of steam production and reduction efficiency in recovery boilers of pulping process. *J. Clean. Prod.* **2020**, *275*, 124103. [[CrossRef](#)]
12. Khadraoui, M.; Khiari, R.; Brosse, N.; Bergaoui, L.; Mauret, E. Combination of Steam Explosion and TEMPO-mediated Oxidation as Pretreatments to Produce Nanofibril of Cellulose from *Posidonia oceanica* Bleached Fibres. *BioResources* **2022**, *17*, 2933–2958. [[CrossRef](#)]
13. Zahra, A.; Gao, S.; Park, J.M.; Shin, S.-J. Impact of Carboxymethylation Pretreatment on the Rheology of Cellulose Nanofiber from Bleached Rice Hull. *J. Korea TAPPI* **2022**, *54*, 63–72. [[CrossRef](#)]
14. Gao, X.; Lim, S.-K.; Song, W.-Y.; Shin, S.-J.; Seong, H.A. Impact of Carboxymethylation Pretreatment on Bleached Rice Hull Nanofiber by Grinding. *J. Korea TAPPI* **2021**, *53*, 146–156. [[CrossRef](#)]
15. Saini, J.K. Lignocellulose-based nanomaterials for diagnostic and therapeutic applications. In *Nanobioanalytical Approaches to Medical Diagnostics*; Woodhead Publishing: Cambridge, UK, 2022; pp. 285–302. [[CrossRef](#)]

16. Yi, T.; Zhao, H.; Mo, Q.; Pan, D.; Liu, Y.; Huang, L.; Xu, H.; Hu, B.; Song, H. From Cellulose to Cellulose Nanofibrils—A Comprehensive Review of the Preparation and Modification of Cellulose Nanofibrils. *Materials* **2020**, *13*, 5062. [[CrossRef](#)]
17. Yu, O.; Kim, K.H. Lignin to Materials: A Focused Review on Recent Novel Lignin Applications. *Appl. Sci.* **2020**, *10*, 4626. [[CrossRef](#)]
18. Lee, D.; Oh, Y.; Yoo, J.K.; Yi, J.W.; Um, M.K.; Park, T. Rheological study of cellulose nanofiber disintegrated by a controlled high-intensity ultrasonication for a delicate nano-fibrillation. *Cellulose* **2020**, *27*, 9257–9269. [[CrossRef](#)]
19. Balea, A.; Monte, M.C.; Fuente, E.; Sanchez-Salvador, J.L.; Tarrés, Q.; Mutjé, P.; Delgado-Aguilar, M.; Negro, C. Fit-for-Use Nanofibrillated Cellulose from Recovered Paper. *Nanomaterials* **2023**, *13*, 2536. [[CrossRef](#)]
20. Ahn, J.; Lee, D.; Youe, W.J.; Lee, B.T.; Lee, T.J.; Seo, J.; Gwon, J. Mechanical Processing Control in Manufacturing Nanofibrillated Cellulose by Interpreting its Rheological Properties. *BioResources* **2022**, *17*, 2906–2916. [[CrossRef](#)]
21. Tyagi, P. Nanocellulose-Based Sustainable Barrier and Antimicrobial Coatings. Ph.D. Thesis, North Carolina State University, Raleigh, NC, USA, 2019.
22. Solala, I.; Iglesias, M.C.; Peresin, M.S. On the potential of lignin-containing cellulose nanofibrils (LCNFs): A review on properties and applications. *Cellulose* **2020**, *27*, 1853–1877. [[CrossRef](#)]
23. Rivière, G. Transformation of Lignin and Lignocellulose into Nanoparticles: Structure-Property Relationship and Applications. Ph.D. Thesis, Aalto University, Espoo, Finland, 2021.
24. Zahra, A.; Lim, S.-K.; Shin, S.-J. Separation of Cellulose from Rice Hull. *J. Korea TAPPI* **2021**, *53*, 28–34. [[CrossRef](#)]
25. Kiemle, D.J.; Stipanovic, A.J.; Mayo, K.E. *Proton NMR Methods in the Compositional Characterization of Polysaccharides*; ACS Publications: Washington, DC, USA, 2004; pp. 122–139. [[CrossRef](#)]
26. Shin, S.J.; Cho, N.S. Conversion factors for carbohydrate analysis by hydrolysis and ¹H-NMR spectroscopy. *Cellulose* **2008**, *15*, 255–260. [[CrossRef](#)]
27. Song, W.-Y. Analysis of Degree of Substitution and Substitution Position from Different Carboxymethylation Reaction Condition. Master's Thesis, Chungbuk National University, Cheongju-si, Republic of Korea, 2018.
28. *ISO 22412*; Particle Size Analysis—Dynamic Light Scattering (DLS). ISO: Geneva, Switzerland, 2008.
29. Abbas, A.; Ansumali, S. Global potential of rice husk as a renewable feedstock for ethanol biofuel production. *BioEnergy Res.* **2010**, *3*, 328–334. [[CrossRef](#)]
30. Ma'arif, A.; Pramudono, B.; Aryanti, N. Lignin isolation process from rice husk by alkaline hydrogen peroxide: Lignin and silica extracted. *AIP Conf. Proc.* **2017**, *1823*, 020013, AIP Publishing LLC. [[CrossRef](#)]
31. Rosado, M.J.; Rencoret, J.; Marques, G.; Gutiérrez, A.; Del Río, J.C. Structural characteristics of the guaiacyl-rich lignins from rice (*Oryza sativa* L.) husks and straw. *Front. Plant Sci.* **2021**, *12*, 640475. [[CrossRef](#)] [[PubMed](#)]
32. Zhao, X.; Zhou, Y.; Zheng, G.; Liu, D. Microwave pretreatment of substrates for cellulase production by solid-state fermentation. *Appl. Biochem. Biotechnol.* **2010**, *160*, 1557–1571. [[CrossRef](#)] [[PubMed](#)]
33. Onyianta, A.J.; Dorris, M.; Williams, R.L. Aqueous morpholine pre-treatment in cellulose nanofibril (CNF) production: Comparison with carboxymethylation and TEMPO oxidisation pre-treatment methods. *Cellulose* **2018**, *25*, 1047–1064. [[CrossRef](#)]
34. Md Azman, S.A.H.; Sagadevan, S.; Ahmad, I.; Kassim, M.H.M.; Imam, S.S.; Nguyen, K.D.; Kaus, N.H.M. Integration of carboxymethyl cellulose isolated from oil palm empty fruit bunch waste into bismuth ferrite as photocatalyst for effective anionic dyes degradation. *Catalysis* **2022**, *12*, 1205. [[CrossRef](#)]
35. Lavoine, N.; Desloges, I.; Dufresne, A.; Bras, J. Microfibrillated cellulose—Its barrier properties and applications in cellulosic materials: A review. *Carbohydr. Polym.* **2012**, *90*, 735–764. [[CrossRef](#)] [[PubMed](#)]
36. Zahra, A.; Lim, S.-K.; Shin, S.-J.; Yeon, I.-J. Properties of Green Tea Waste as Cosmetics Ingredients and Rheology Enhancers. *Appl. Sci.* **2022**, *12*, 12871. [[CrossRef](#)]
37. Masruchin, N.; Amanda, P.; Kusumaningrum, W.B.; Suryanegara, L.; Nuryawan, A. Particle size distribution and yield analysis of different charged cellulose nanofibrils obtained by TEMPO-mediated oxidation. In *IOP Conference Series: Earth and Environmental Science, Proceedings of the 9th International Symposium for Sustainable Humanosphere, Bogor, Indonesia, 28–29 October 2019*; IOP Publishing: Bristol, UK, 2020; Volume 572, p. 012045. [[CrossRef](#)]
38. Zhai, L.; Kim, H.C.; Kim, J.W.; Kim, J. Simple centrifugal fractionation to reduce the size distribution of cellulose nanofibers. *Sci. Rep.* **2020**, *10*, 11744. [[CrossRef](#)]
39. Liao, J.; Pham, K.A.; Breedveld, V. Rheological characterization and modeling of cellulose nanocrystal and TEMPO-oxidized cellulose nanofibril suspensions. *Cellulose* **2020**, *27*, 3741–3757. [[CrossRef](#)]
40. Song, W.Y.; Juhn, S.; Gwak, J.H.; Shin, S.J.; Seong, H.A. Width Length Measurement of Cellulose Nanofibril by Nanoparticle Analyzer: Comparison with TEM Image Analysis. *J. Korea TAPPI* **2019**, *51*, 121–127. [[CrossRef](#)]
41. Balea, A.; Blanco, A.; Delgado-Aguilar, M.; Monte, M.C.; Tarres, Q.; Mutjé, P.; Negro, C. Nanocellulose Characterization Challenges. *BioResources* **2021**, *16*, 4382–4410. [[CrossRef](#)]
42. Boyd, R.D.; Pichaimuthu, S.K.; Cuenat, A. New approach to inter-technique comparisons for nanoparticle size measurements; using atomic force microscopy, nanoparticle tracking analysis and dynamic light scattering. *Colloids Surf. A Physicochem. Eng. Asp.* **2011**, *387*, 35–42. [[CrossRef](#)]
43. Eshel, G.; Levy, G.J.; Mingelgrin, U.; Singer, M.J. Critical evaluation of the use of laser diffraction for particle-size distribution analysis. *Soil Sci. Soc. Am. J.* **2004**, *68*, 736–743. [[CrossRef](#)]
44. Siró, I.; Plackett, D. Microfibrillated cellulose and new nanocomposite materials: A review. *Cellulose* **2010**, *17*, 459–494. [[CrossRef](#)]

45. Iwamoto, S.; Lee, S.H.; Endo, T. Relationship between aspect ratio and suspension viscosity of wood cellulose nanofibers. *Polym. J.* **2014**, *46*, 73–76. [[CrossRef](#)]
46. Han, J.; Zhou, C.; Wu, Y.; Liu, F.; Wu, Q. Self-assembling behavior of cellulose nanoparticles during freeze-drying: Effect of suspension concentration, particle size, crystal structure, and surface charge. *Biomacromolecules* **2013**, *14*, 1529–1540. [[CrossRef](#)]
47. Sofla, M.R.K.; Brown, R.J.; Tsuzuki, T.; Rainey, T.J. A comparison of cellulose nanocrystals and cellulose nanofibres extracted from bagasse using acid and ball milling methods. *Adv. Nat. Sci. Nanosci. Nanotechnol.* **2016**, *7*, 035004. [[CrossRef](#)]

Disclaimer/Publisher’s Note: The statements, opinions and data contained in all publications are solely those of the individual author(s) and contributor(s) and not of MDPI and/or the editor(s). MDPI and/or the editor(s) disclaim responsibility for any injury to people or property resulting from any ideas, methods, instructions or products referred to in the content.